Inorg. Chem. **2005**, *44*, 9288–9292

NH/π Interaction in a Spin-Crossover Complex $[Fe^{II}(HL^{Me})_2](BPh_4)_2 \cdot 2CH_3CN$ (BPh_4^- = Tetraphenylborate; HL^{Me} = 2-Methylimidazol-4-yl-methylideneamino-2-ethylpyridine)

Shinobu Arata,[†] Haruna Torigoe,[†] Tomotaka Iihoshi,[†] Naohide Matsumoto,*[,†] Françoise Dahan,[‡] and Jean-Pierre Tuchagues[‡]

Department of Chemistry, Faculty of Science, Kumamoto University, Kurokami 2-39-1, Kumamoto 860-8555, Japan, and Laboratoire de Chimie de Coordination du CNRS, UP 8241, 205 Route de Narbonne, 31077 Toulouse cedex, France

Received July 21, 2005

Three Fe^{II} complexes, $[Fe(HL^R)_2](BPh_4)_2 \cdot$solvent (R = H, Me, Ph), were synthesized, where BPh_4^- = tetraphenylborate and HL^R = 2-substituted-imidazol-4-yl-methylideneamino-2-ethylpyridine. The magnetic susceptibility measurements in 5–300 K revealed that $[Fe(HL^H)_2](BPh_4)_2 \cdot H_2O$ (**1**), $[Fe(HL^{Me})_2](BPh_4)_2 \cdot 2CH_3CN$ (**2**), and $[Fe(HL^{Ph})_2](BPh_4)_2 \cdot CH_3CN$ (**3**) are low-spin (LS), spin-crossover (SC), and high-spin (HS) Fe^{II} complexes, respectively, indicating that the spin state can be effectively tuned by the bulkiness of the substituent. Complex **2** shows a steep SC around 250 K, where it assumes a cyclic structure of $\{[Fe(HL^{Me})_2]BPh_4\}_2$ constructed by four NH/π bonds between the imidazole group and the phenyl ring of BPh_4^- in the HS state and a deformed structure with NH/π bonds and linear $CH_3CN \cdots HN$ hydrogen bonds at the terminals in the LS state.

Introduction

Linear hydrogen bonds between −OH or −NH groups and proton acceptors with highly electronegative atoms are one of the most important interactions in modern chemistry from molecular biology to material design.[1] The weaker CH/π and NH/π interactions also play important roles in supramolecular chemistry and protein biochemistry.[2] The NH/π interaction has been found in several proteins and in hemoglobin−drug complexes.[3] The investigation of crystal databases revealed that there are NH/π or CH/π interactions in a number of crystal structures.[4] Tsuzuki et al. and others evaluated the amplitude of the CH/π and NH/π interactions by high-level ab initio calculations and demonstrated that the calculated interaction energy (i.e., −2.22 kcal/mol for a benzene−ammonia complex) is about half of the linear hydrogen-bond energy.[5]

Spin crossover (SC) between the low-spin (LS) and high-spin (HS) states is induced by an external perturbation, such as temperature, pressure, or light irradiation.[6] It is now well established that the interactions between SC sites govern the SC properties such as steepness, hysteresis, and the LIESST (light-induced excited spin-state trapping) effect. Such SC behaviors have been found in polymeric SC compounds with bridging ligands[7] and mononuclear SC compounds exhibiting intermolecular interactions such as hydrogen bonding[8] and

* To whom correspondence should be addressed. E-mail: naohide@aster.sci.kumamoto-u.ac.jp. Fax: +81-96-342-3390.
[†] Kumamoto University.
[‡] Laboratoire de Chimie de Coordination du CNRS Toulouse.

(1) Jeffrey, G. A.; Saenger, W. *Hydrogen Bonding in Biological Structures*; Springer: New York, 1991.
(2) Rodham, D. A.; Suzuki, S.; Suenram, R. D.; Lovas, F. L.; Dasgupta, S.; Goddard, W. A., III; Blake, G. A. *Nature* **1993**, *362*, 735−737.
(3) Fong, T. M.; Cascieri, M. A.; Yu, H.; Bansal, A.; Swain, C.; Strader, C. D. *Nature* **1993**, *362*, 350−353.
(4) Umezawa, Y.; Tsuboyama, S.; Takahashi, H.; Uzawa, J.; Nishio, M. *Tetrahedron* **1999**, *55*, 10047−10056.
(5) Tsuzuki, S.; Honda, K.; Uchimura, T.; Mikami, M.; Tanabe, K. *J. Am. Chem. Soc.* **2000**, *122*, 3746−3753 and 11450−11458.
(6) (a) Gütlich, P.; Goodwin, H. A. *Spin Crossover in Transition Metal Compounds I−III*, *Topics in Current Chemistry*; Springer: New York, 2004; 233−235. (b) Gütlich, P.; Hauser, A.; Spiering, H. *Angew. Chem., Int. Ed. Engl.* **1994**, *33*, 2024−2054.
(7) (a) Kahn, O.; Martinez, J. C. *Science* **1998**, *279*, 44. (b) Real, J. A.; Andres, E.; Munoz, M. C.; Julve, M.; Granier, T.; Bousseksou, A.; Varret, F. *Science* **1995**, *268*, 265−267.
(8) (a) Sunatsuki, Y.; Ikuta, Y.; Matsumoto, N.; Ohta, H.; Kojima, M.; Iijima, S.; Hayami, S.; Maeda, Y.; Kaizaki, S.; Dahan, F.; Tuchagues, J.-P. *Angew. Chem., Int. Ed.* **2003**, *42*, 1614−1618. (b) Ikuta, Y.; Ooidemizu, M.; Yamahata, Y.; Yamada, M.; Osa, S.; Matsumoto, N.; Iijima, S.; Sunatsuki, Y.; Kojima, M.; Dahan, F.; Tuchagues, J.-P. *Inorg. Chem.* **2003**, *42*, 7001−7017. (c) Yamada, M.; Ooidemizu, M.; Ikuta, Y.; Osa, S.; Matsumoto, N.; Iijima, S.; Kojima, M.; Dahan, F.; Tuchagues, J.-P. *Inorg. Chem.* **2003**, *42*, 8406−8416.

10.1021/ic051215i CCC: $30.25
Published on Web 11/05/2005

$\pi-\pi$ stacking.[9] Reger et al. synthesized Fe^{II} complexes with alkyne coupled poly(pyrazoyl)borate ligands and demonstrated that the long-range interaction from the CH/π interaction at the rather terminal part is effective to control the SC behavior.[10] Combination between SC and liquid crystalline properties has been also investigated recently.[11] The investigation of NH/π interaction in the SC phenomenon should be important because the NH/π interaction has been found in several proteins and in hemoglobin−drug complexes. Here, we report the SC complex $[Fe^{II}(HL^{Me})_2](BPh_4)_2\cdot 2CH_3CN$ (**2**) (BPh_4^- = tetraphenylborate; HL^{Me} = 2-methylimidazol-4-yl-methylideneamino-2-ethylpyridine), in which NH/π interactions play a role in causing a steep SC behavior.

Results and Discussion

Synthesis and Characterization of $[Fe(HL^H)_2](BPh_4)_2\cdot H_2O$ (1), $[Fe(HL^{Me})_2](BPh_4)_2\cdot 2CH_3CN$ (2), and $[Fe(HL^{Ph})_2](BPh_4)_2\cdot CH_3CN$ (3). It should be noted that the Fe^{II} complexes were synthesized in air. The tridentate ligand was prepared by the 1:1 condensation reaction of 2-substituted-4-formylimidazole and 2-(2-aminoethyl)pyridine in methanol (substituent = H, Me, and Ph), and the resulting ligand solution was used for the syntheses of the Fe^{II} complexes. The Fe^{II} complexes were prepared by mixing the methanol solution of the tridentate ligand, $Fe^{II}Cl_2\cdot 4H_2O$, and $NaBPh_4$ with 2:1:2 molar ratios, where crude products immediately precipitated and were collected by suction filtration. Crude products were recrystallized from acetonitrile in air. Well-grown crystals involving solvent molecules were obtained from slow crystallization at room temperature. The formulas for $[Fe(HL^H)_2](BPh_4)_2\cdot H_2O$ (**1**), $[Fe(HL^{Me})_2](BPh_4)_2\cdot 2CH_3CN$ (**2**), and $[Fe(HL^{Ph})_2](BPh_4)_2\cdot CH_3CN$ (**3**) were confirmed by the elemental and crystal-structure analyses. Compounds $[Fe(HL^H)_2](BPh_4)_2\cdot H_2O$ (**1**) and $[Fe(HL^{Ph})_2](BPh_4)_2\cdot CH_3CN$ (**3**) show no thermochromism and assume red-brown and yellow colors, respectively, at ambient temperature. Compound $[Fe(HL^{Me})_2](BPh_4)_2\cdot 2CH_3CN$ (**2**) show a thermochromism from yellow-brown at ambient temperature to deep red at liquid nitrogen temperature. The infrared spectra show two characteristic intense bands at ca. 1605 and 1630 cm^{-1},[12] assignable to the C=N stretching vibration of the Schiff-base ligands whose relative intensity depends on the size of substituents. For the H substituent, the band at ca. 1605 cm^{-1} assumes a stronger absorption than that at ca. 1630 cm^{-1}, while for substituents Me and Ph, the band at ca. 1605 cm^{-1} assumes a weaker absorption than that at ca. 1630 cm^{-1}.

Magnetic Properties. The magnetic susceptibilities of the crystalline samples were measured in the temperature range of 5−300 K at the 1 K min^{-1} sweeping mode under an applied magnetic field of 0.5 T. The sample was quickly cooled to 5 K from room temperature, and the magnetic susceptibility was measured while the temperature was increased from 5 to 300 K in the first run. Subsequently, the magnetic susceptibility was measured while the temperature was lowered from 300 to 5 K as the second run. The magnetic behaviors of the first and second runs are nearly the same, indicating that there is no frozen-in effect and no hysteresis. Figure 1 shows the $\chi_M T$ versus T plots for the crystal samples of **1**−**3**. The $\chi_M T$ value of **1** is 0.6 cm^3 K mol^{-1} at 300 K and decreases moderately from 0.6 cm^3 K mol^{-1} at 300 K to 0 cm^3 K mol^{-1} at 5 K, indicating that **1** is a LS Fe^{II} complex ($S = 0$). The $\chi_M T$ value of **3** is constant in the 300−50 K temperature range at ca. 3.8 cm^3 K mol^{-1} and decreases steeply in the lowest-temperature region, indicating that **3** is a HS Fe^{II} complex ($S = 2$). The $\chi_M T$ value of **2** changes abruptly from the HS value to the LS value around 250 K, indicating that **2** is a SC complex. The above results demonstrate that the spin state can be tuned effectively by the selection of the substituent at the 2-substituted-4-formylimidazole moiety. The order of the substituent of H, methyl, and phenyl groups is not the order of the electron reduction effect but the order of the bulkiness.

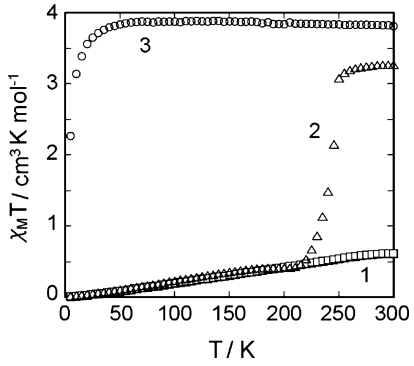

Figure 1. Magnetic behavior of crystalline samples for $[Fe^{II}(HL^H)_2](BPh_4)_2\cdot H_2O$ (**1**), $[Fe^{II}(HL^{Me})_2](BPh_4)_2\cdot 2CH_3CN$ (**2**), and $[Fe^{II}(HL^{Ph})_2](BPh_4)_2\cdot CH_3CN$ (**3**), in the form of $\chi_M T$ versus T plots on the warming mode. The samples were quickly cooled from 300 to 5 K, and $\chi_M T$ was successively measured upon warming from 5 to 300 K and upon cooling from 300 to 5 K. For three complexes, the magnetic behaviors on the cooling and warming modes are not different. The crystalline samples were used without grinding for the measurements.

The magnetic behavior of **2** is described in more detail. When the temperature is decreased from 300 K, the $\chi_M T$ value is constant in the temperature range of 300−250 K at ca. 3.2 cm^3 K mol^{-1}, then decreases steeply between 250 and 230 K to ca. 0.5 cm^3 K mol^{-1} at 220 K, and finally decreases moderately to ca. 0.0 cm^3 K mol^{-1} at 5 K. The constant $\chi_M T$ value of ca. 3.2 cm^3 K mol^{-1} at 250−300 K is close to that expected for HS Fe^{II} ($S = 2$) complexes. The minimum value of 0 cm^3 K mol^{-1} at 5 K is compatible with that reported for LS Fe^{II} ($S = 0$) complexes. The most striking feature is the steepness of the present SC behavior around 250 K, which most likely results from some cooperative effects between SC Fe^{II} sites. Another interesting point is that the SC behavior depends on the condition of the sample. When the crystals were ground to yield a powder, the $\chi_M T$ value did not show a steep trend but showed a

(9) (a) Hayami, S.; Gu, Z.; Shiro, M.; Einaga, Y.; Fujishima, A.; Sato, O. *J. Am. Chem. Soc.* **2000**, *122*, 7126. (b) Hayami, S.; Gu, Z.; Yoshiki, H.; Fujishima, A.; Sato, O. *J. Am. Chem. Soc.* **2001**, *123*, 11644.
(10) Reger, D. L.; Gardinier, J. R.; Gemmill, W. R.; Smith, M. D.; Shahin, A. M.; Long, G. J.; Rebbouh, L.; Grandjean, F. *J. Am. Chem. Soc.* **2005**, *127*, 2303−2316 and references therein.
(11) Galyametdinov, Y.; Ksenofontov, V.; Prosvirin, A.; Ovchinnikov, I.; Ivanova, G.; Gütlich, P.; Haase, W. *Angew. Chem.* **2001**, *113*, 4399−4401.
(12) Nakamoto, K. In *Infrared and Raman Spectra of Inorganic and Coordination Compounds*, 5th ed.; John Wiley and Sons: New York, 1997; Part B, Chapter III-14.

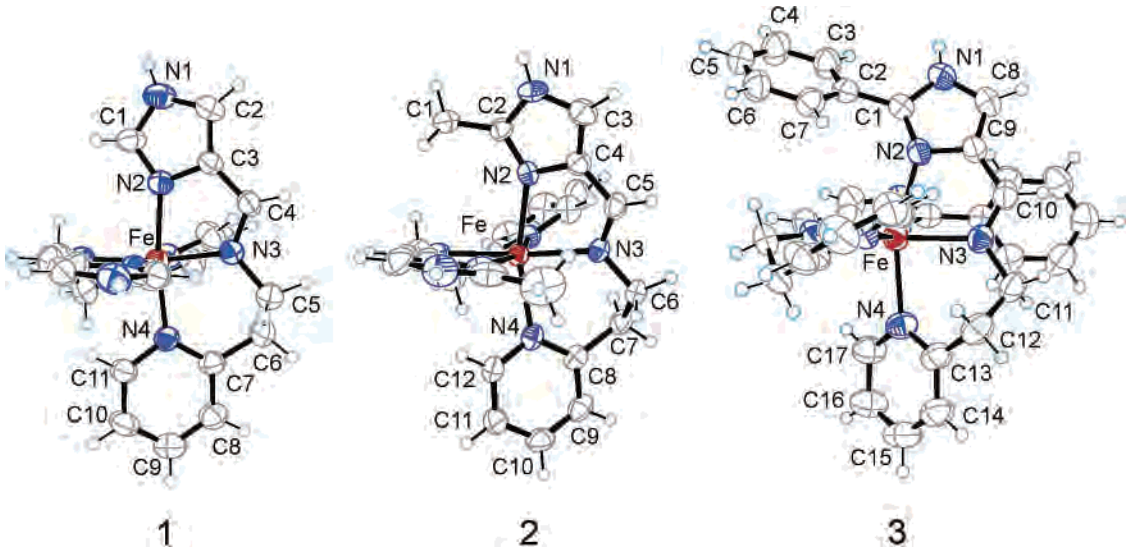

Figure 2. The molecular structures of the cationic part of **1** (LS state at 293 K), **2** (HS state at 260 K), and **3** (HS state at 293 K) with the selected atom numbering schemes.

Table 1. Selected Bond Lengths (Å) and Angles (deg) for $[Fe^{II}(HL^{H})_2](BPh_4)_2 \cdot H_2O$ (**1**), $[Fe^{II}(HL^{Ph})_2](BPh_4)_2 \cdot CH_3CN$ (**3**), and $[Fe^{II}(HL^{Me})_2](BPh_4)_2 \cdot 2CH_3CN$ at 260 K (**2a**) and 110 K (**2b**)

	1	**3**	**2a**	**2b**
Fe−N(2)	1.9644(13)	2.2252(15)	2.1948(19)	1.9880(15)
Fe−N(3)	1.9395(13)	2.1501(16)	2.1764(19)	1.9641(14)
Fe−N(4)	1.9973(13)	2.2149(17)	2.2100(18)	2.0366(14)
Fe−N(6)	1.9705(12)	2.2439(16)	2.1950(17)	1.9978(14)
Fe−N(7)	1.9372(12)	2.1718(16)	2.1425(17)	1.9470(13)
Fe−N(8)	2.0050(13)	2.1903(17)	2.1892(19)	2.0275(13)
N(2)−Fe−N(3)	79.86(6)	76.53(7)	80.39(6)	76.22(6)
N(2)−Fe−N(4)	171.51(5)	161.47(7)	169.25(6)	160.80(6)
N(2)−Fe−N(6)	91.91(5)	86.00(7)	86.02(6)	81.76(6)
N(2)−Fe−N(7)	90.64(5)	101.01(7)	95.82(6)	101.78(6)
N(2)−Fe−N(8)	89.85(5)	91.60(7)	91.54(6)	93.94(6)
N(3)−Fe−N(4)	91.77(6)	85.33(7)	89.85(6)	85.79(6)
N(3)−Fe−N(6)	91.53(5)	98.72(7)	95.09(5)	100.83(6)
N(3)−Fe−N(7)	167.61(5)	174.62(7)	174.84(6)	176.98(7)
N(3)−Fe−N(8)	97.04(5)	99.12(7)	93.79(5)	97.64(6)
N(4)−Fe−N(6)	89.67(5)	93.13(7)	90.41(6)	95.31(6)
N(4)−Fe−N(7)	97.84(5)	96.74(7)	93.64(6)	95.92(6)
N(4)−Fe−N(8)	89.83(5)	95.03(7)	93.60(6)	95.07(6)
N(6)−Fe−N(7)	80.78(5)	76.24(7)	81.10(6)	76.56(6)
N(6)−Fe−N(8)	171.43(5)	160.91(7)	170.27(6)	159.39(6)
N(7)−Fe−N(8)	90.82(5)	85.67(7)	89.79(6)	84.70(6)
N(1)···X	2.984(2)[a]	3.056(3)[b]	−	3.117(2)[c]

[a] N(1)···O(1). [b] N(1)···N(9). [c] N(1)···N(10).

gradual and incomplete SC behavior, suggesting that the cooperative interaction is weak.

Crystal Structures. The molecular structures of the cationic part of **1**−**3** are shown in Figure 2, together with the selected atom numbering schemes. Relevant bond distances and angles as well as the intermolecular hydrogen bond distances are given in Table 1. Since the magnetic susceptibility data demonstrate that **1** and **3** are in the LS and HS states in the whole temperature range, respectively, the single-crystal X-ray analyses of **1** and **3** were performed only at 293 K. Each Fe^{II} ion is in an octahedral coordination environment and coordinated by N_6 donor atoms of two tridentate Schiff-base ligands. The Fe−N distances of **1** are in the range of 1.937(1)−2.005(1) Å, which are typical for LS Fe^{II} complexes with similar nitrogen donor atoms. On the other hand, those of **3** are in the range of 2.150(1)−2.244(1) Å, which are typical for HS Fe^{II} complexes. The average Fe−N distances of **1** and **3** are 1.969 and 2.199 Å, respectively. The N−Fe−N bond angles of **1** are much closer to those of a regular octahedron than those of **3**, as given in Table 1. In the crystal structure of **1**, one of the two imidazole groups per complex cation is hydrogen bonded to the crystal water O(1) with a hydrogen-bond distance of N(1)···O(1) = 2.984(2) Å and another imidazole group contacts incompletely to a phenyl group through a NH/π interaction. There are no further intermolecular contacts. In the crystal structure of **3**, one of two imidazole groups per complex cation is hydrogen bonded to the acetonitrile molecule with a hydrogen-bond distance of N(1)···N(9) = 3.056(3) Å and another imidazole group contacts to a phenyl group through a NH/π interaction. There are no further intermolecular contacts. It should be noted that there are no intermolecular interactions between the Fe sites in both complexes **1** and **3**.

Since the magnetic susceptibility data of **2** show an abrupt SC around 250 K, the crystal structures were solved at 260 and 110 K, to reveal the detailed structures in the HS and LS Fe^{II} states. The crystallographic data in the HS and LS states are similar to each other, and no crystallographic phase transition occurs during the spin transition. The unit cell volume of 3247.1(5) $Å^3$ at 260 K is reduced to 3137.4(4) $Å^3$ at 110 K. The reduction of 3.4% is slightly smaller than the values reported for other SC Fe^{II} complexes with similar N_6 donor atoms (ca. 5%). The Fe^{II} ion is coordinated by two tridentate HL^{Me} ligands and assumes an octahedral coordination environment. On the basis of the Fe−N bond distances and N−Fe−N bond angles, the spin state can be well identified. At 260 K, the Fe−N distances are in the range of 2.143(2)−2.210(2) Å, typical for HS Fe^{II} bound to imine and imidazole nitrogen atoms. At 110 K, the Fe−N distances are in the range of 1.988(2)−2.037(1) Å, typical for LS Fe^{II}. The average Fe−N distance decreases from 2.184 Å at 260 K to 1.993 Å at 110 K by 0.19 Å, which is comparable to previously reported values (ca. 0.2 Å). The N−Fe−N bond

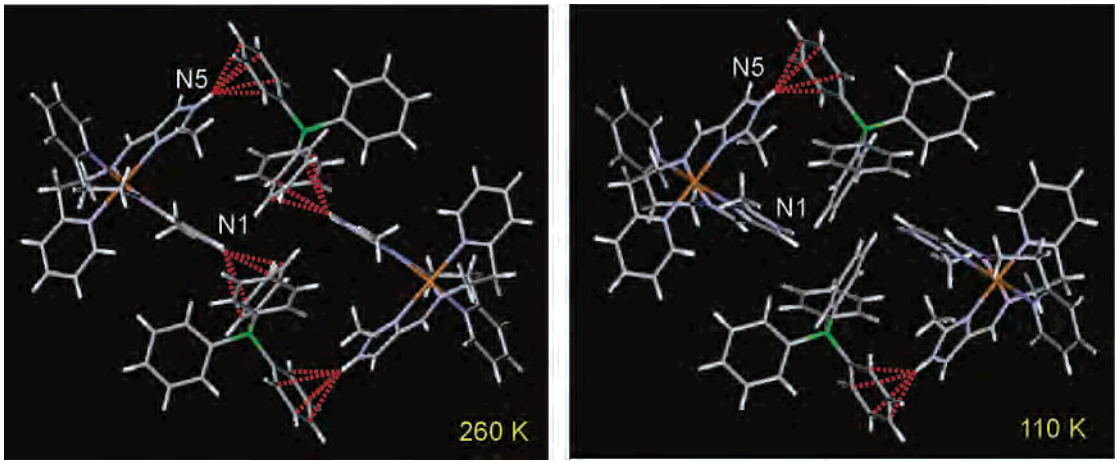

Figure 3. Aggregated structures of $[Fe(HL^{Me})_2](BPh_4)_2 \cdot 2CH_3CN$ (**2**) at 260 K (left) and 110 K (right). The cyclic structure at 260 K results from NH/π bonds between the imidazole NH group of $[Fe^{II}(HL^{Me})_2]^{2+}$ and a phenyl group of BPh_4^- anion. At 110 K, the linear hydrogen bond between $CH_3CN\cdots$HN(imidazole group) appears instead of one NH/π bond to produce a deformed structure.

angles change drastically during the spin transition, and are getting closer to those of a regular octahedron in the LS state, as shown in Table 1.

Figure 3 shows a cyclic structure of **2a** at 260 and the deformed structure **2b** at 110 K, respectively. The cyclic structure at 260 K consists of two $[Fe^{II}(HL^{Me})_2]^{2+}$ cations and two BPh_4^- anions. The structure is constructed by an NH/π interaction between the imidazole NH group of $[Fe^{II}(HL^{Me})_2]^{2+}$ and a phenyl group of one BPh_4^- anion. Two imidazole groups per $[Fe^{II}(HL^{Me})_2]^{2+}$ and two phenyl rings per BPh_4^- participate in the formation of the cyclic structure because of the NH/π bonds, where the distances of the imidazole nitrogen and central position of the phenyl ring are 3.125 and 3.287 Å for $N(1)\cdots P_A$ and $N(5)\cdots P_B$, respectively. One of two crystallographically unique BPh_4^- anions is involved in the cyclic structure. The two acetonitrile molecules show no significant intermolecular contact in the HS state. A careful crystallographic investigation demonstrated that there are no other intermolecular interactions but the NH/π ones. At 110 K, one of the two NH/π bonds per cationic molecule, $N(5)\cdots P_B$, is shortened to 3.151 Å at 110 K from 3.287 Å at 260 K, but the $N(1)\cdots P_A$ distance is elongated from 3.125 Å at 260 K to 3.675 Å at 110 K, suggesting a rupture of N(1)H/π bond. Instead of the N(1)H/π bond, the imidazole group N(1) becomes closer to an acetonitrile molecule with a slightly longer hydrogen bond distance of $N(1)\cdots N(10) = 3.117(2)$ Å. Consequently, at 110 K the cyclic structure constructed by four NH/π bonds is disrupted to give a deformed structure with two NH/π bonds and two $CH_3CN\cdots$HN hydrogen bonds at the terminals, as shown in Figure 3.

Concluding Remarks. A combination of SC and NH/π interactions has been considered to play an important role in the light of its biological relevance, since both properties are simultaneously observed in numerous heme proteins. The present result gives an example that NH/π interactions may play a significant role in the SC phenomenon.

Experimental Section

General and Materials. The synthesis of the Fe^{II} complexes was carried out in air. All chemicals and solvents were reagent grade and were obtained from Tokyo Kasei Co. Ltd. and Wako Pure Chemical Industries Ltd. They were used for the synthesis without further purification.

$[Fe(HL^H)_2](BPh_4)_2 \cdot H_2O$ (1). A solution of 2-(2-aminoethyl)-pyridine (0.245 g, 2 mmol) in 5 mL of methanol was added to a solution of 4-formylimidazole (0.195 g, 2 mmol) in 10 mL of methanol. The resulting solution was stirred on a hot plate at 50 °C for 15 min. The ligand solution was used for the synthesis of the Fe^{II} complex without isolation of the ligand. A solution of $Fe^{II}Cl_2 \cdot 4H_2O$ (0.200 g, 1 mmol) in 10 mL of methanol was added to the ligand solution (2 mmol). A solution of tetraphenylborate (0.684 g, 2 mmol) in 10 mL of methanol was added to the mixture. The resulting solution was stirred on a hot plate at 50 °C for 10 min and then left overnight. An orange powder was collected and recrystallized from a minimum amount of acetonitrile. Red brown crystals were collected by suction filtration. Yield: 0.938 g (84%). Anal. Calcd for $[Fe^{II}(HL^H)_2](BPh_4)_2 \cdot H_2O$: C, 74.35; H, 6.06; N, 9.91. Found: C, 74.19; H, 5.95; N, 10.00. IR (KBr): $\nu_{C=N}$ 1607.1, 1633.2 cm^{-1}.

$[Fe^{II}(HL^{Me})_2](BPh_4)_2 \cdot 2CH_3CN$ (2). The complex was prepared in a manner similar to that used to prepare **1** using 2-methyl-4-formylimidazole instead of 4-formylimidazole. Yellow-brown crystals were collected by suction filtration. Yield: 0.527 g (44%). Anal. Calcd for $[Fe^{II}(HL^{Me})_2](BPh_4)_2 \cdot 2CH_3CN$: C, 75.76; H, 6.19; N, 11.62. Found: C, 75.87; H. 6.04; N, 11.70. IR(KBr): $\nu_{C=N}$ 1605.7, 1629.9 cm^{-1}.

$[Fe(HL^{Ph})_2](BPh_4)_2 \cdot CH_3CN$ (3). The complex was prepared in a manner similar to that used to prepare **1** using 2-phenyl-4-formylimidazole instead of 4-formylimidazole. Yellow crystals were collected by suction filtration. Yield: 1.01 g (78%). Anal. Calcd for $[Fe(HL^{Ph})_2](BPh_4)_2 \cdot CH_3CN$: C, 78.33; H, 5.87; N, 9.79. Found: C, 78.13; H, 5.81; N, 9.96. IR(KBr): $\nu_{C=N}$ 1605.2, 1633.4 cm^{-1}.

Physical Measurements. Elemental C, H, and N analyses were carried out at the Center for Instrumental Analysis of Kumamoto University. Infrared spectra were recorded on a Perkin-Elmer FT-IR PARAGON 1000 spectrometer using KBr disks at ambient temperature. Magnetic susceptibilities were measured using a MPMS5 SQUID (Quantum Design) in the 5−300 K temperature

Table 2. X-ray Crystallographic Data for $[Fe^{II}(HL^{H})_2](BPh_4)_2 \cdot H_2O$ (**1**), $[Fe^{II}(HL^{Ph})_2](BPh_4)_2 \cdot CH_3CN$ (**3**), $[Fe^{II}(HL^{Me})_2](BPh_4)_2 \cdot 2CH_3CN$ at 260 K (**2a**) and at 110 K (**2b**)

	1	**3**	**2a**	**2b**
formula	$C_{70}H_{66}B_2FeN_8O$	$C_{84}H_{75}B_2FeN_9$	$C_{76}H_{74}B_2FeN_{10}$	$C_{76}H_{74}B_2FeN_{10}$
fw	1112.78	1288.00	1204.92	1204.92
cryst syst	monoclinic	monoclinic	triclinic	triclinic
space group	$P2_1/c$ (No. 14)	$P2_1/c$ (No. 14)	$P\bar{1}$ (No. 2)	$P\bar{1}$ (No. 2)
a (Å)	19.7613(18)	20.4076(14)	12.9932(13)	12.9678(12)
b (Å)	13.7470(10)	17.5345(17)	22.873(2)	22.231(2)
c (Å)	22.652(2)	20.0717(13)	11.5710(7)	11.3416(7)
α (deg)	90	90	96.821(10)	95.260(9)
β (deg)	98.622(10)	102.204(8)	105.182(10)	103.596(10)
γ (deg)	90	90	97.599(12)	96.039(12)
V (Å^3)	6084.2(9)	7020.1(9)	3247.1(5)	3137.4(4)
Z	4	4	2	2
T (K)	293	293	260	110
D_{calcd} (Mg m^{-3})	1.215	1.219	1.232	1.275
μ(Mo Kα) (mm^{-1})	0.298	0.267	0.285	0.294
no. collected	49203	55310	27966	26819
no. unique	11917	13553	15692	15118
no. of obsd reflns[a]	6124	7559	5801	8007
R1[b] obsd, all	0.0376, 0.0572	0.0379, 0.0732	0.0366, 0.0632	0.0349, 0.0603
wR2[c] obsd, all	0.0542, 0.0584	0.0759, 0.0853	0.0528, 0.0924	0.0485, 0.0615
S	0.814	0.814	0.771	0.784
(Δ/ρ) min,max (e Å^{-3})	0.295, −0.366	0.201, −0.333	0.429, −0.336	0.379, −0.293

[a] Data with $F_o > 4\sigma(F_o)$. [b] $R1 = \sum||F_o| - |F_c||/\sum|F_o|$. [c] $wR2 = [\sum w(|F_o^2| - |F_c^2|)^2/\sum w|F_o^2|^2]^{1/2}$.

range at the 1 K/min sweeping mode under an applied magnetic field of 0.5 T. The calibration was done with palladium metal. Corrections for diamagnetism were made using Pascal's constants.[13]

Crystallographic Data Collection and Structure Analyses. A crystal of **1** (red square plate, 0.20 × 0.20 × 0.05 mm^3) and a crystal of **3** (yellow block, 0.40 × 0.35 × 0.30 mm^3) were used for the single-crystal X-ray diffraction study at 293 K. Each crystal was mounted on a Stoe Imaging Plate Diffractometer System (IPDS) using a graphite monochromated Mo Kα radiation ($\lambda = 0.71073$ Å). The crystal-to-detector distance was 70 mm (max 2θ value 52.1°). Numerical absorption corrections were applied for **1** ($T_{min-max} = 0.5136-0.7298$) and **3** ($T_{min-max} = 0.5594-0.6743$).

A crystal of **2** (yellow-brown plate, 0.50 × 0.20 × 0.10 mm^3) was mounted on an Oxford-Diffraction Xcalibur diffractometer[14] using graphite monochromated Mo Kα radiation ($\lambda = 0.71073$ Å) and equipped with an Oxford Instruments Cryojet cooler device. Data were collected at 260 and 110 K. Gaussian absorption corrections could be applied ($T_{min-max} = 0.6478-0.8524$ at 260 K and $T_{min-max} = 0.6647-0.8258$ at 110 K).

The structures were solved using SHELXS-97[15] and refined on F^2 by full-matrix least-squares using SHELXL-97[16] with anisotropic displacement parameters for all non-hydrogen atoms except the disordered acetonitrile molecule in **2** at 260 K. Refinement was achieved with H atoms introduced in calculations using the riding model, except those bonded to O(1) in **1** which were not found. Isotropic U_H values were 1.1 times higher than those of the atom to which they are bonded. The atomic scattering factors and anomalous dispersion terms were taken from the standard compilation.[17] Crystal data collection and refinement parameters are given in Table 2.

Acknowledgment. This work was supported in part by a Grant-in-Aid for Science Research (No. 16205010) from the Ministry of Education, Science, Sports, and Culture, Japan.

Note Added after ASAP Publication. This article was released ASAP on November 5, 2005, with a bar missing over the 1 in $P\bar{1}$ in the fourth column of Table 2. The correct version was posted on November 9, 2005.

Supporting Information Available: X-ray crystallographic file in CIF format for **1**, **2**, and **3**. This material is available free of charge via the Internet at http://pubs.acs.org.

IC051215I

(13) Kahn, O. *Molecular Magnetism*; VCH: Weinheim, Germany, 1993.
(14) (a) Watkin, D. J.; Prout, C. K.; Carruthers, J. R.; Betteridge, P. W. *CRYSTALS*, issue 10; Chemical Crystallography Laboratory: Oxford, U.K. (b) *CRYSALIS*, version 170; Oxford-Diffraction: Oxford, U.K., 2002.
(15) Sheldrick, G, M, *SHELXS-97. Program for Crystal Structure Solution*; University of Göttingen: Göttingen, Germany, 1990.
(16) Sheldrick, G. M. *SHELXL-97. Program for the Refinement of Crystal Structures from Diffraction Data*; University of Göttingen: Göttingen, Germany, 1997.
(17) *International Tables for Crystallography*; Kluwer Academic Publishers: Dordrecht, The Netherlands, 1992; Vol. C.